Journal of Solid State Chemistry 182 (2009) 2279–2284

Contents lists available at ScienceDirect

Journal of Solid State Chemistry

journal homepage: www.elsevier.com/locate/jssc

Decorating multi-walled carbon nanotubes with nickel nanoparticles for selective hydrogenation of citral

Yuechao Tang [a], Dong Yang [a], Feng Qin [b], Jianhua Hu [a], Changchun Wang [a,*], Hualong Xu [b,*]

[a] Key Laboratory of Molecular Engineering of Polymers (Ministry of Education), Department of Macromolecular Science and Advanced Materials Laboratory, Fudan University, Shanghai 200433, China

[b] Department of Chemistry, Fudan University, Shanghai 200433, China

ARTICLE INFO

Article history:
Received 31 March 2009
Received in revised form
12 May 2009
Accepted 27 May 2009
Available online 2 June 2009

Keywords:
MWNTs
Ni nanoparticles
Surface modification
Catalyst
Hydrogenation of citral

ABSTRACT

The nanocomposites of multi-walled carbon nanotubes (MWNTs) decorated with nickel nanoparticles were conveniently prepared by a chemical reduction of nickel salt in the present of poly(acrylic acid) grafted MWNTs (PAA-*g*-MWNTs). Due to the strong interaction between Ni^{2+} and –COOH, PAA-*g*-MWNTs became an excellent supporting material for Ni nanoparticles. The morphology and distribution of Ni nanoparticles on the surface of MWNTs were greatly influenced by the reduction temperatures, the experimental results also showed that the distribution of Ni nanoparticles was greatly improved while the MWNTs were modified by poly(acrylic acid) (PAA). The hydrogenation activity and selectivity of MWNTs decorated with Ni nanoparticles (Ni-MWNTs) for α, β-unsaturated aldehyde (citral) were also studied, and the experimental results showed that the citronellal, an important raw material for flavoring and perfumery industries, is the favorable product with a percentage as high as 86.9%, which is 7 times higher than that of catalyst by Ni-supported active carbon (Ni-AC).

1. Introduction

The outstanding physical properties, such as the ultra-high surface area, high mechanical strength but ultra-light weight, high chemical, and thermal stability, make carbon nanotubes (CNTs) as an ideal candidate for supporting material, and arouse intensive research on loading of drugs [1], quantum dots [2], catalysts [3,4], magnetic particles [5], and so on [6]. To date, many metals, e.g. Pt, Au, Pd, Ag, Ru, as well as Ni, have been successfully deposited onto the surface of CNTs to obtain the nanocomposites of CNTs decorated with metal or metal oxide nanoparticles [7–15], which endow CNTs with new properties and expand the application scope of CNTs. These nanocomposites showed remarkable advantage in improving sensor properties [16,17] and catalytic efficiency [18,19].

Due to the relatively high catalytic activity and low price compared to precious metals, Ni is an ideal candidate for fabrication of metal nanoparticles-CNTs nanocomposites in application of catalyst [20], hydrogen storage [21], electrochemical capacitor [22], and so on. So far, several methods had been used to prepare Ni nanoparticles decorated CNTs (Ni-CNTs). Kim et al. [23] have prepared Ni-MWNTs nanocomposites with 6 wt% Ni loading by immerging multi-walled carbon nanotubes (MWNTs) into a Ni nitrate acetone solution, then dried at 60 °C and heat-treated with H_2 flow. Arai et al. [24] deposited Ni nanoparticles onto MWNTs through an electro-evaporation process. Besides of the above methods, chemical reduction method has been proved to be a versatile, simple and highly efficient method to deposit metal nanoparticles onto CNTs [6]. Liu et al. decorated pristine MWNTs with Ag nanoparticles through a traditional silver mirror reaction. Ag nanoparticles with a diameter less than 50 nm were successfully deposited onto the sidewall of MWNTs [25]. Li et al. have prepared Pt nanoparticles decorated MWNTs nanocomposites through chemically reducing Pt ions in the presence of surface-oxidized MWNTs, and the Pt nanoparticles were homogenously dispersed on the outer surface of MWNTs with a diameter in the range of 2–5 nm [26]. Recently, we prepared Pt nanoparticles decorated MWNTs (Pt-MWNTs) by a chemical reduction method, using poly(acrylic acid) (PAA) functionalized MWNTs as supporting materials [27]. The density and uniformity of Pt nanoparticles deposited on MWNTs were found greatly influenced by the PAA grafting density, the surface functionality of CNTs is a significant factor to control the nucleation, growth and distribution of the metal nanoparticles supported on CNTs.

Among most of the functional groups, carboxyl group (–COOH) is customarily used as nucleation site for the deposition of metal nanoparticles [28] and can be introduced to CNTs surface through various methods [29,30]. Recently, we reported a 'fishing' process to prepare poly(acrylic acid) covalently grafted MWNTs (PAA-*g*-MWNTs), containing many of carboxyl groups on the outer surface of MWNTs [31]. In this paper, Ni nanoparticles were

* Corresponding authors. Fax: +86 21 65640293.
E-mail address: ccwang@fudan.edu.cn (C. Wang).

0022-4596/$ - see front matter © 2009 Elsevier Inc. All rights reserved.
doi:10.1016/j.jssc.2009.05.036

successfully deposited onto PAA-*g*-MWNTs surface by chemical reduction using hydrazine hydrate ($N_2H_4 \cdot H_2O$) as reducing agent, the schematic preparation process was shown in Scheme 1. Experimental results indicated that the Ni nanoparticles were uniformly distributed on the outer surface of PAA-*g*-MWNTs. This nanocomposite has been used for catalytic hydrogenation of citral (3,7-dimethyl-2,6-octadienal), and the experimental result showed that it possessed high catalytic activity (conversion ≈ 73%) and very high monohydrogenation selectivity (appropriately 91%) at 80 °C.

2. Experimental

2.1. Materials

Pristine multi-walled carbon nanotubes (purity >95%), produced by chemical vapor deposition (CVD) method, were purchased from Shenzhen Nanotech Port Co. Ltd. Active carbon (AC) (purity >85%) was purchased from Shanghai Qinghua Chemical Reagent Corporation. 2,2-azobisisobutyronitrile (AIBN) (purity >98%), acrylic acid (AA) (purity >98%), acetone (purity >98%), ethylene glycol (EG) (purity >98%), hydrazine hydrate (purity >95%), and nickel chloride (purity >95%) were all purchased from Shanghai Chemical Reagent Corporation. Citral (purity >95%), with a 1:1 mixture of Z form and E form, was purchased from Sinopharm Chemical Reagent Co. Ltd. AIBN was recrystallized from ethanol before use. All the other reagents were used as received.

2.2. Preparation of poly(acrylic acid) grafted MWNTs

PAA-*g*-MWNTs were prepared according to our previous work [31]. Typically, 0.1 g MWNTs were added into 100 mL acetone. After sonication for 10 min, 1.0 g AA was added into and the solution was purged with dry nitrogen for 30 min to remove oxygen, finally 0.05 g AIBN was added. The reaction was kept at 65 °C for 5 h. After that, the solution was filtered through a 0.45 μm polyvinylidene fluoride (PVDF) membrane, and washed with deionized water for 5 times, to give PAA-*g*-MWNTs as a black solid. The content of PAA in PAA-*g*-MWNTs evaluated by thermogravimetric analysis (TGA) was about 12 wt% (see supporting information, Figure S1).

2.3. Preparation of Ni nanoparticles decorated MWNTs (Ni-MWNTs)

Ni-MWNTs were prepared through a chemical reduction process, using hydrazine hydrate as reducing agent, sodium hydroxide as catalyst and ethylene glycol as solvent. For a typical reaction, 30 mg PAA-*g*-MWNTs were charged into 50 mL EG solution, containing 62 mg $NiCl_2 \cdot 6H_2O$, 27 mg NaOH, and 0.26 g hydrazine hydrate. The reaction was kept at 80 °C for 2 h, then Ni-MWNTs were centrifuged out, and washed with deionized water for 5 times. Finally, the Ni-MWNTs were dispersed and stored in ethanol. For comparison, Ni-supported active carbon (Ni-AC) was prepared by impregnating active carbon with $NiCl_2 \cdot 6H_2O$ aqueous solution, dried in 100 °C and finally reduced by 1 M KBH_4 at room temperature.

2.4. Selective hydrogenation of citral

The hydrogenation of citral was carried out in 100 mL FCZ-1 autoclave with magnetic coupled stirrer at a constant stirring rate of 500 rpm. A 1.0 g of citral was firstly mixed with 50 mL ethanol, then 0.14 g Ni-MWNTs nanocomposites (24 wt% Ni loading, see supporting imformation S2) was charged into the reactor. Hydrogen was bubbled through the solution to remove the traces

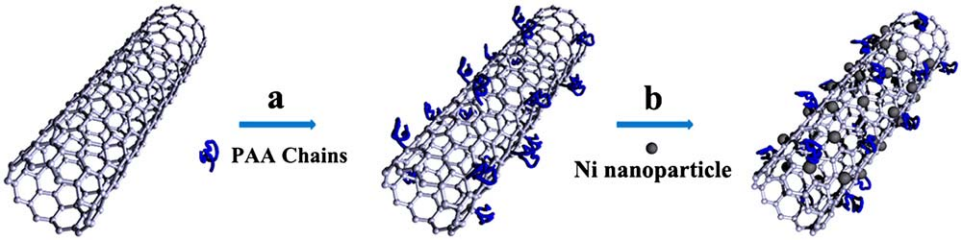

Scheme. 1. Schematic preparation process of Ni nanoparticles decorated MWNTs: (a) a 'fishing' process to prepare poly(acrylic acid) covalently grafted MWNTs and (b) a chemical reduction process to prepared Ni nanoparticles decorated MWNTs.

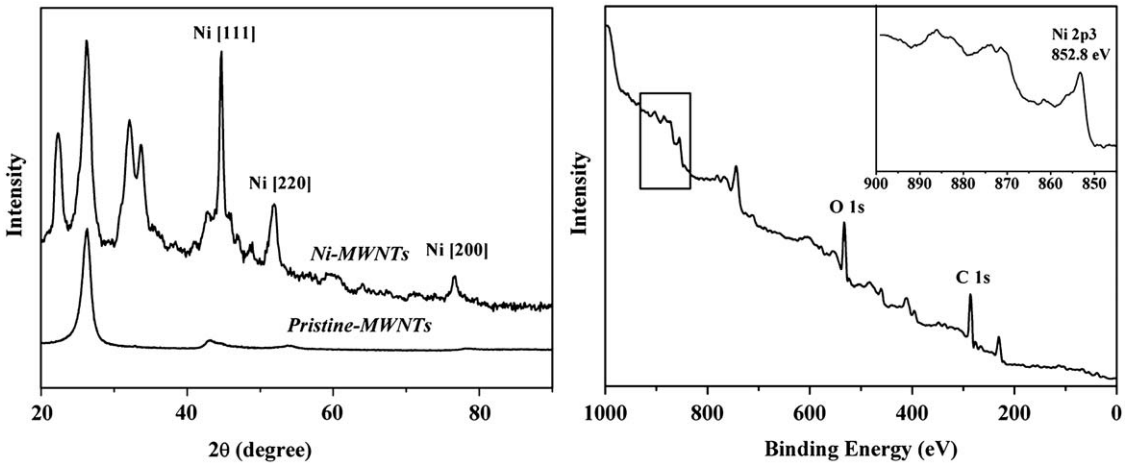

Fig. 1. (a) The XRD spectra of Ni-MWNTs and pristine MWNTs and (b) the XPS spectrum of Ni-MWNTs.

of air for 30 min. The reaction was kept at 80 °C and 1.0 MPa H_2 pressure for 2 h. Reaction products were filtered and analyzed by gas chromatograph (GC).

2.5. Characterization

Transmission electron microscopy (TEM) investigation was carried out on a Hitachi H600 electron microscope, the accelerating voltage was 75 kV. For the sample preparation, the Ni-MWNTs composites were dispersed in deionized water under sonication for 2 min, then one drop of the solution was added on a holey copper grid, and the excess of MWNTs suspension was removed. FT-IR spectroscopy was carried out on a NEXUS-470 spectrometer using KBr pallets. Weight loss of the sample in elevated temperature in air or nitrogen atmosphere was carried out on a TGA instrument (Perkin-Elmer Pyris-1 series) under nitrogen atmosphere at a scan rate of 20 °C/min. X-ray photoelectron spectroscopy (XPS) was performed on a RBD upgraded PHI-5000C ESCA system (Perkin-Elmer) using Al-monochromatic X-ray at a power of 25 W with an X-ray-beam diameter of 10 mm, and a pass energy of 29.35 eV. The pressure of analyzer chamber was maintained below 5×10^{-8} Pa during the measurement. The binding energy was calibrated using the C 1 s photoelectron peak at 284.6 eV as the reference. X-ray diffraction (XRD) analyses were carried out on a PANalytical XMPert powder X-ray diffractometer with Cu$K\alpha$ radiation (40 kV, 40 mA). A scan rate of 10°/min was applied to record the patterns in the 2θ range of 40°–90°. The reaction products of citral were analyzed by gas chromatography (GC, HP 5890) equipped with a 30 m SE-54 capillary column and a flame ionization detector. The injector temperature was 260 °C, and the detector column temperature was increased from 80 to 260 °C with a ramp rate of 15 °C/min.

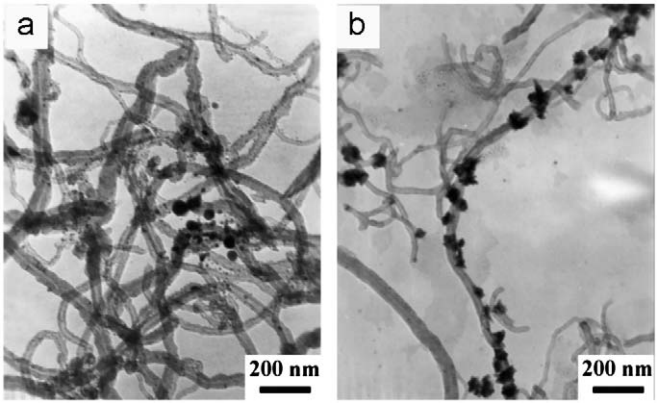

Fig. 2. TEM images of: (a) Ni nanoparticles deposited on pristine MWNTs and (b) Ni nanoparticles deposited on PAA-*g*-MWNTs.

3. Results and discussion

3.1. Preparation of Ni nanoparticles decorated MWNTs (Ni-MWNTs)

In our experiments, a simple chemical reduction method was used for preparation of Ni nanoparticles decorated MWNTs. The as-prepared Ni-MWNTs were characterized by X-ray diffraction and X-ray photoelectron spectroscopy. As seen in Fig. 1a, comparison with pristine MWNTs, the XRD spectrum of Ni-MWNTs showed three characteristic peaks at 44.7°, 51.6°, and 76.9°, assigned to Ni(111), Ni(220), and Ni(200), respectively [32], which demonstrated that the Ni nanoparticles deposited on the surface of MWNTs were face centered cubic (fcc) structure. As shown in Fig. 1b, the binding energy located at 852.8 eV is for $2p_{3/2}$ of Ni nanoparticles deposited onto PAA-*g*-MWNTs, which is consistent with a metallic state of nickel [33], lower than those of nickel oxides, i.e. NiO (853.3–854.8 eV) or Ni_2O_3 (855.6–857.1 eV) [34], indicating that the nickel element in nanoparticles was in zero-valence state.

At the same time, a control experiment was conducted to deposit Ni nanoparticles onto the outer surface of pristine MWNTs under the similar deposition condition of PAA-*g*-MWNTs, the detailed result was showed in Fig. 2a. From the TEM image of Fig. 2a, it could be seen that Ni nanoparticles were aggregated together to form large clusters. While utilizing PAA-*g*-MWNTs as the supporting materials, it was found that Ni nanoparticles were uniformly distributed on the outer surface of PAA-*g*-MWNTs (Fig. 2b). This result indicates that the functionalization of MWNTs with PAA is critical for the well deposited Ni nanoparticles on the surface of MWNTs, the grafted PAA chains afford not only solubility for MWNTs, but also large numbers of carboxyl groups for integrating of Ni nanoparticles. Actually, even after sonicated by a bath sonicator (60 kHz) for 10 min, no obvious detaching or aggregating of Ni nanoparticles was detected. But for pristine MWNTs, Ni nanoparticles were attached so weakly that the nanoparticles would easily fall down when ultrasonication or violence agitation was applied.

3.2. Effect of temperature on the deposition of Ni nanoparticles

As shown in Fig. 3, the distribution of Ni nanoparticles deposited onto PAA-*g*-MWNTs can be greatly influenced by changing the temperatures in deposition process. The nanocomposites with well-dispersed Ni nanoparticles on the surface of PAA-*g*-MWNTs could be obtained at 80 °C (Fig. 3b), while the Ni

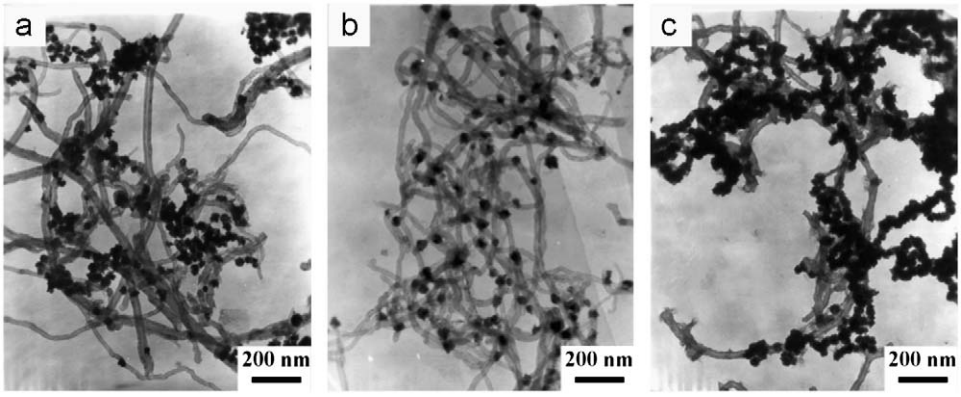

Fig. 3. TEM images of Ni-MWNTs prepared in different temperature: (a) 60 °C, (b) 80 °C, and (c) 100 °C.

nanoparticles were aggregated seriously when temperature was further increased to 100 °C (Fig. 3c). In this reaction system, the nickel ions can be reduced by hydrazine, and the trace amount of NaOH is very helpful in accelerating the reduction rate. At the same time, the reduction temperature is also a very important parameter in determining the reduction rate. Compared with high temperature, low temperature in deposition process leads to slower reduction rate and fewer nuclei, finally fewer Ni nanoparticles would be formed. When the reduction temperature was low as 80 °C, the reduction rate is slow and a small number of nuclei would be formed. Due to the –COOH groups on the surface of PAA-*g*-MWNTs were the favorite nucleation sites for Ni nanoparticles, the formed Ni nuclei which were few in number would attach onto the out surface of PAA-*g*-MWNTs, as a result, Ni nanoparticles would be well deposited on to the surface of PAA-*g*-MWNTs just as shown in Fig. 3b. When the temperature was increased to 100 °C, the reduction rate would be increased as well, and a relatively large number of nuclei would be formed at a short time compared with that in 80 °C. Due to the number of –COOH on the surface of PAA-*g*-MWNTs which were available for the deposition of the formed Ni nuclei was insufficient, some nuclei and nickel nanoparticles would be formed in solution. As a kind of permanent magnetic materials, each nickel particle has an inherent self-generated magnetic field [35]. Driven by this magnetic field, the Ni particles would prefer aggregating along the magnetic force lines. Thus, the Ni nanoprticles supported on MWNTs at 100 °C presents a bead-like morphology. If the above reason is real, then the density of Ni nanoparticles on the surface of PAA-*g*-MWNTs prepared at 60 °C (Fig. 3a) will be lower than that at 80 °C (Fig. 3b), but the fact is denial. Actually, if we examine the TEM image (Fig. 3a) carefully, we can find that the nanoparticles attach to the surface of PAA-*g*-MWNTs directly is rare, most of the nanoparticles aggregate together around the nanoparticles attached on the surface of PAA-*g*-MWNTs, the main reason is that the nucleation rate of the nickel nanoparticles was slow at low temperature, and the concentration of free Ni ion in the reaction solution is high. It is well known that Ni possess self-catalysis property at low temperature [36], the existed metal Ni would promote rapid reduction of Ni^{2+} ions in solution which enable more Ni nanoparticles to form and assemble around the original Ni nanoparticles on the surface, then many Ni nanoparticles aggregated together and supported on the surface of PAA-*g*-MWNTs, just as shown in Fig. 3a.

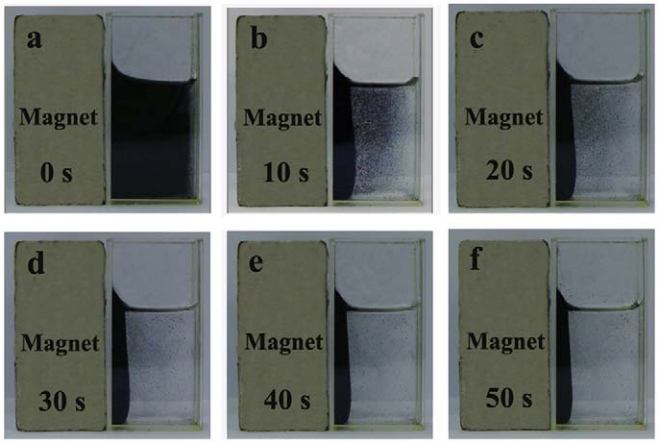

Fig. 4. Magnetic response of Ni-MWNTs.

3.3. Magnetic response of Ni-decorated MWNTs

The Ni-MWNTs nanocomposites were found to be magnetic responsive, due to the decoration of Ni nanoparticles. As shown in Fig. 4, Ni-MWNTs can be totally separated from the solution within approximately 50 s while applying a magnetic field on the side of the vial. This result also hinted that the Ni nanoparticles were tightly bound to PAA-*g*-MWNTs. Besides, the magnetic

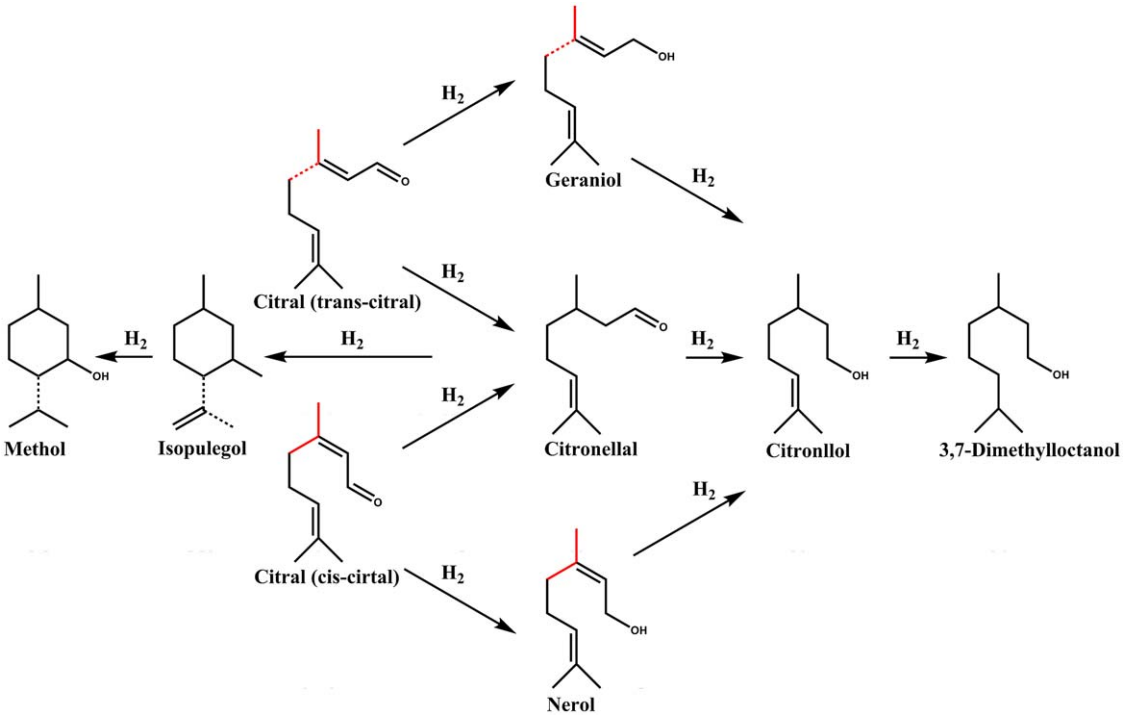

Scheme. 2. Illustration of citral hydrogenation.

Table 1
Catalytic results of citral hydrogenation over Ni-MWNTs and Ni-AC catalysts.

Catalyst	Conversion (%)	Monohydrogenation selectivity (%)	Selectivity distribution (%)				
			Citronellal	Citronellol	Nerol	Geraniol	other
Ni-MWNTs	72.7	91.2	86.9	5.9	0.0	4.3	2.9
Ni-AC	90.0	56.4	10.9	8.6	18.3	27.2	34.0

Catalysis condition: $T = 80\,^{\circ}C$; $P_{H2} = 1.0$ MPa; $m_{Ni/MWNTs} = 0.14$ g ($m_{Ni/AC} = 0.28$ g); $m_{citral} = 1.0$ g; $V_{ethanol} = 50$ mL; 500 rpm; 2 h.

responsive behavior is also a quite useful property, which can lead to a quick separation of the Ni-MWNTs nanocomposites' catalyst from the reaction system when the catalytic hydrogenation reaction was finished.

3.4. Selective hydrogenation of citral

The evolution of selective hydrogenation of citral is shown in scheme 2. The reaction network, considering all the possible hydrogenation routes that citral may undergo, is shown in Scheme 2. The geraniol/nerol isomers are obtained by selectively hydrogenating C=O functional group of the citral, while citronellal is obtained by the selective hydrogenation of the conjugated C=C bond. In turn, citronellol can be obtained by the selective hydrogenation of the citronellal C=O group or from the C=C bond of geraniol/nerol.

The ratio of monohydrogenation products (geraniol, nerol, and citronellal) to the overall hydrogenation products is defined as monohydrogenation selectivity. The products of monohydrogenation of citral, including geraniol, nerol and citronellal, are important in flavoring and perfumery industries. However, it remains challenging to produce citronellal selectively vs other monohydrogenation products. The catalytic activities, monohydrogenation selectivity and distribution of products for hydrogenation of citral were studied in this part, the detailed results were listed in Table 1. In Table 1, we can find that the monohydrogenation selectivity of citral catalyzed by Ni-MWNTs (Ni nanoparticles deposited on PAA-*g*-MWNTs) were sharply higher, approximately 91.2% with 72.7% conversion, while in the control experiment using activated carbon (Ni-AC) decorated with Ni nanoparticles as catalyst, it exhibited a 56.4% monohydrogenation selectivity and 90.0% conversion (see Table 1). Besides, the citronellal is the favorable product with a percentage as high as 86.9% for Ni-MWNTs, which is 7 times higher than that of catalyst by Ni-supported active carbon.

Just as we know, larger surface area is beneficial to high activity and conversion [37], which is consistent with the case of the high conversion of Ni-AC nanocomposite. Due to the smaller size of the Ni nanoparticles on Ni-AC nanocomposite compared to the Ni nanoparticles deposited on the PAA-*g*-MWNTs, Ni-AC nanocomposite showed an apparent higher conversion. Additionally, the difference in the product selectivity between the two catalysts is more notable. The Ni-MWNTs nanocomposite favored the hydrogenation of C=C which result in citronellal as the main product with a total selectivity of 86.9%, while the Ni-AC catalyst showed no apparent favored hydrogenation route showing a selectivity of citronellal about 10.9%, nerol about 18.3%, geraniol about 27.2%. (GC data, see supporting information, Figure S3 and S4). The high selectivity to citronellal may be attributed to the spiny shaped structure of Ni nanoparticles (Fig. 5), whose facet exposed to the reaction system has an apparently favor in citronellal. Currently, we are optimizing the Ni nanoparticles deposition reactions to further control the particle distribution, morphology, size in the aim to achieve both high yield and high selectivity of citronellal production.

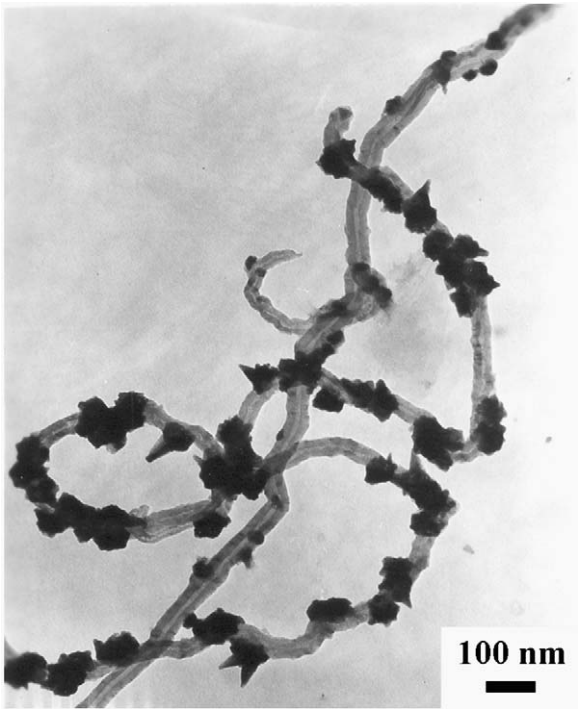

Fig. 5. TEM image of PAA-*g*-MWNTs decorated with Ni nanoparticles with spiny appearance.

4. Conclusion

In summary, PAA-*g*-MWNTs, synthesized by *in situ* free radical polymerization of PAA in poor solvent, were utilized to support Ni nanoparticles by a chemical reduction method. The grafted PAA on the surface of MWNTs can greatly improve the shape and distribution of the deposited Ni nanoparticles. The morphology and distribution of Ni nanoparticles can also be controlled by changing the temperatures in deposition process. These Ni-MWNTs nanocomposites were magnetic responsive, which is merit for separation of catalysts from the hydrogenation system. The hydrogenation experiment of the Ni-MWNTs nanocomposite shows a fairly good catalytic selectivity in citral hydrogenation favoring citronellal as the main product.

Acknowledgments

This work was supported by National Science Foundation of China (Grant nos. 20374012 and 50873029), China Postdoctoral Science Foundation Funded Project (20080440569), National Science Foundation for Distinguished Young Scholars of China (50525310), and Shanghai Leading Academic Discipline Project (B113).

Appendix A. Supplementary material

Supplementary data associated with this article can be found in the online version at doi:10.1016/j.jssc.2009.05.036.

References

[1] Z. Liu, X. Sun, R.N. Nakayama, H. Dai, ACS Nano 1 (2007) 50.
[2] S. Chaudhary, J.H. Kim, K.V. Singh, M. Ozkan, Nano. Lett. 4 (2004) 2415.
[3] V. Georgakilas, D. Gournis, V. Tzitzios, L. Pasquato, D.M. Guldi, M. Prato, J. Mater. Chem. 17 (2007) 2679.
[4] L. Chen, G.Z. Hu, G.J. Zou, S.J. Shao, X.L. Wang, Electrochem. Commun. 11 (2009) 504.
[5] G. Korneva, H.H. Ye, Y. Gogotsi, D. Halverson, G. Friedman, J.C. Bradley, K.G. Kornev, Nano. Lett. 5 (2005) 879.
[6] X.G. Hua, S.J. Dong, J. Mater. Chem. 18 (2008) 1279.
[7] L.M. Ang, T.S.A. Hor, G.Q. Xu, C.H. Tung, S.P. Zhao, J.L.S. Wang, Chem. Mater. 11 (1999) 2115.
[8] B. Xue, P. Chen, Q. Hong, J. Lin, K.L. Tan, J. Mater. Chem. 11 (2001) 2378.
[9] J. Chen, M. Wang, B. Liu, Z. Fan, K. Cui, Y. Kuang, J. Phys. Chem. B 110 (2006) 11775.
[10] J.S. Ye, H.F. Cui, X. Liu, T.M. Lim, W.D. Zhang, F.S. Sheu, Small 1 (2005) 560.
[11] N. Lordi, V. Yao, J. Wei, Chem. Mater. 13 (2001) 733.
[12] Y. Lin, X. Cui, C. Yen, C.M. Wa, J. Phys. Chem. B 109 (2005) 14410.
[13] Y. Wang, X. Xu, Z. Tian, Y. Zong, H. Cheng, C. Lin, Chem. Eur. J. 12 (2006) 2542.
[14] D.J. Guo, H.L. Li, Carbon 43 (2005) 1259.
[15] T.M. Day, P.R. Unwin, N.R. Wilson, J.V. Macpherson, J. Am. Chem. Soc. 127 (2005) 10639.
[16] J.N. Xie, S.Y. Wang, L. Aryasomayajula, V.K. Varadan, Nanotechnology 18 (2007) 065503.
[17] J.Y. Liu, Z. Guo, F.L. Meng, Y. Jia, J.H. Liu, J. Phys. Chem. 112 (2008) 6119.
[18] G. Girishkumar, K. Vinodgopal, P.V. Kamat, J. Phys. Chem. B 108 (2004) 19960.
[19] K. Nikolaos, E.T. Georgia, E. Fabrizio, R. Petra, R. Nikitas, T. Nikos, J. Phys. Chem. C 112 (2008) 13463.
[20] S.H. Wu, D.H. Chen, J. Colloid Interface Sci. 259 (2003) 282.
[21] C.T. Hsieh, Y.W. Chou, J.Y. Lin, Int. J. Hydrogen Energy 32 (2007) 3457.
[22] C.T. Hsieh, Y.W. Chou, W.Y. Chen, J. Solid State Electrochem. 12 (2008) 663.
[23] H.S. Kim, H. Lee, K.S. Han, J.H. Kim, M.S. Song, M.S. Park, J.Y. Lee, J.K. Kang, J. Phys. Chem. B 109 (2005) 8983.
[24] S. Arai, M. Endo, N. Kaneko, Carbon 42 (2004) 641.
[25] Y.Y. Liu, J. Tang, X.Q. Chen, W. Chen, G.K.H. Pang, J.H. Xin, Carbon 44 (2006) 381.
[26] W. Li, C. Liang, W. Zhou, J. Qiu, Z. Zhou, G. Sun, Q. Xin, J. Phys. Chem. B 107 (2003) 6292.
[27] G.Q. Guo, F. Qin, D. Yang, C.C. Wang, H.L. Xu, S. Yang, Chem. Mater. 20 (2008) 2291.
[28] R.V. Hull, L. Li, Y.C. Xing, C.C. Chusuei, Chem. Mater. 18 (2006) 1780.
[29] D. Tasis, N. Tagmatarchis, A. Bianco, M. Prato, Chem. Rev. 106 (2006) 1105.
[30] D. Yang, J.H. Hu, C.C. Wang, Carbon 44 (2006) 3161.
[31] G.Q. Guo, D. Yang, C.C. Wang, S. Yang, Macromolecules 39 (2006) 9035.
[32] D. Fatemeh, F. Zeinab, S.N. Salavati, J. Alloys Compd. 476 (2009) 797.
[33] S.O. Grim, L.J. Matienzo, W.E. Swartz, J. Am. Chem. Soc. 94 (1972) 5116.
[34] C.D. Wagner, W.M. Riggs, L.E. Davis, Handbook of X-ray Photoelectron Spectroscopy, Perkin-Elmer, Minnesota, 1979.
[35] C.H. Gong, J.T. Tian, T. Zhao, Z.S. Wu, Z.J. Zhang, Mater. Res. Bull. 44 (2009) 35.
[36] Q. Peng, J.C. Spagnola, G.N. Parsonsa, J. Electrochem. Soc. 155 (2008) 580.
[37] F. Qin, W. Shen, C.C. Wang, H.L. Xu, Catal. Commun. 9 (2008) 2095.